Journal of
NANOSTRUCTURES
JNS
NANOSTRUCTURES
JNS.kashanu.ac.ir

Microwave-assisted Synthesis of $MgFe_2O_4$-ZnO Nanocomposite and Its Photo-catalyst Investigation in Methyl Orange Degradation

G. Nabiyouni *[,a], D. Ghanbari [b], J. Ghasemi [a], A. Yousofnejad [a]

[a] *Department of Physics, Faculty of Science, Arak University, Arak 38156-88349, Iran*

[b] *Young Researchers and Elite Club, Arak Branch, Islamic Azad University, Arak, Iran*

Article history:
Received 05/08/2015
Accepted 27/08/2015
Published online 01/09/2015

Keywords:
Microwave
$MgFe_2O_4$-ZnO
Nanocomposites

**Corresponding author:*
E-mail address:.
G-nabiyouni@araku.ac.ir
Phone: +98 86 34173401-5
Fax: +98 86 34173406

Abstract

In this work firstly $MgFe_2O_4$ nanoparticles were synthesized via a microwave-assisted method. The product was calcinated at 900 ºC for 2h. At the second step zinc oxide shell was synthesized on the ferrite under ultrasonic waves. Properties of the product were examined by X-ray diffraction pattern (XRD), scanning electron microscope (SEM) and Fourier transform infrared (FT-IR) spectroscopy. Vibrating sample magnetometer (VSM) shows nanoparticles exhibit ferromagnetic behavior. The photo-catalytic behavior of $MgFe_2O_4$-ZnO nanocomposite was evaluated using the degradation of organic dyes aqueous solution under ultraviolet (UV) light irradiation. The results show that $MgFe_2O_4$-ZnO nanocomposites have applicable magnetic and photo-catalytic performance.

1. Introduction

$MgFe_2O_4$ has exhibited unique magnetic properties because of its low toxicity, good biocompatibility and tunable magnetic properties. Magnesium ferrite have received considerable attention in various areas such as catalysis, magnetic refrigeration systems, drug delivery and turgeting, heat transfer applications, cancer therapy, enzyme immobilization and magnetic cell separation [1].

Various methods to eliminate pollutants compounds from wastewater have been reported in the previous published articles; among them, the advanced oxidation processes, in which the photo-degradation processes are included. These processes consist in the decomposition of organic molecules interacting with both, an UV or visible light as well as the interaction with a

photo-catalyst material, in order to get CO_2 and H_2O as final products [2]. Several semiconductor materials have been reported in the literatureas such as TiO_2 (effective and most frequently mentioned) ZrO_2, WO_3, ZnO, ZnS, SnO_2, Fe_2O_3, as well as large number of binary, ternary and quaternary mixed oxides.

There is an increasing interest in magnetic ferrite nanoparticles because of their broad applications in several technological fields including permanent magnets, magnetic fluids, drug delivery, microwave devices, and high density information storage [3–5]. Ferrite has been widely studied because it possesses excellent chemical stability and suitable mechanical hardness. In addition to the precise control on the composition and structure of $MgFe_2O_4$ different chemical and physical synthesis methods, such as precipitation, sol-gel, hydrothermal are used to produce ferrite. Among the reported methods, the microwave method is an efficient way to production of ultrafine and mono-dispersed magnetic powder [6-10].

Ultrasonic emethod operated under ambient conditions. Ultrasonic waves propagate through the solution causing alternating high and low pressure in the liquid media. Ultrasonic irradiation caused cavitation in a liquid medium where the formation, growth and implosive collapse of bubbles occurred. The collapse of bubbles with short lifetimes produces intense local heating and high pressure. These localized hot spots can generate a temperature of around 5000 °C and a pressure of over 1800 kPa and can drive many chemical reactions [11-16].

A variety of synthesis strategies for ferrites nanostructure materials have been described. Microwave method as a simple, effective and novel route has been developed to prepare nanostructures[16-18].

In the present work, $MgFe_2O_4$ nanoparticles and $MgFe_2O_4$-ZnO nanocomposites were synthesized by a surfactant-free microwave method without using inert atmosphere. The obtained samples were characterized by scanning electron microscopy and X-ray diffraction pattern. The magnetic properties were investigated using a vibrating sample magnetometer. Magnetic photo-catalysts have gained much attention because those can easily be seperated from polluted waters by applying a simple magnetic field.

2 Experimental

2.1. Materials and Instruments

$Fe(NO_3)_3$ $9H_2O$, Zn(OAc) $4H_2O$, NaOH and NH_3 were purchased from Merck Company. All of the chemicals were used as received without further purifications. XRD patterns were recorded by a Philips, X-ray diffracttometer using Ni-filtered Cu K_α radiation. For SEM images the samples were coated by a very thin layer of Au to make the sample surface conductor and prevent charge accumulation, and obtaining a better contrast. Room temperature magnetic properties were investigated using a vibrating sample magnetometer (VSM, made by Meghnatis Daghigh Kavir Company) in an applied magnetic field sweeping between ±10000 Oe.

A multiwave ultrasonic generator (Sonicator 3000; Bandeline, MS 73, Germany), equipped with a converter/transducer and titanium oscillator (horn), 1.25×10^{-2} m in diameter, surface area of ultrasound irradiating face: 1.23×10^{-4} m^2, operating at 20 kHz, was used for the

ultrasonic irradiation and the horn was operated at 50% amplitude. All ultrasonication experiments were carried out at ultrasonic power between 84–125 mW measured by calorimeter.

2.2. Synthesis of nanoparticles and nanocomposites

0.1 mol of $Mg(NO_3)_2$ $6H_2O$ and 0.2 mol of $Fe(NO_3)_3$ $9H_2O$ is dissolved in 100 ml of propylene glycol. 15 ml of NaOH solution (1M) is slowly added to the solution under microwave irradiation 900W and 5min until pH:10. The product was calcind at 900°C for 2h. A black precipitate is obtained confirming the synthesis of $MgFe_2O_4$. The precipitate of $MgFe_2O_4$ is then centrifuged and rinsed with distilled water, followed by being left in an atmosphere environment to dry. Fig.1a shows the schematic diagram for experimental setup used in this microwave method.

In step 2 nanoparticles were dispersed in water solution and zinc acetate was dissolved in the solution simultaneously. 4 ml of ammonia was added to solution under sonication (100 W, 15 min, Fig 1b). The precipitate of $MgFe_2O_4$-ZnO is then centrifuged and rinsed with distilled water.

3. Results and discussion

The XRD pattern of $MgFe_2O_4$ nanoparticles is shown in Fig. 2. The pattern of as-prepared $MgFe_2O_4$ nanoparticles is indexed as a pure cubic phase which is very close to the literature values (JCPDS No. 71-1232). Space group of magnesium ferrite is Fd3m. The narrow sharp peaks indicate that the $MgFe_2O_4$ nanoparticles are well crystallized.

The crystallite size measurements were also carried out using the Scherrer equation,

$$D_c=K\lambda/\beta Cos\theta$$

Where β is the width of the observed diffraction peak at its half maximum intensity (FWHM), K is the shape factor, which takes a value of about 0.9, and λ is the X-ray wavelength (CuK_α radiation, equals to 0.154 nm). The estimated crystallite size was about 16 nm.

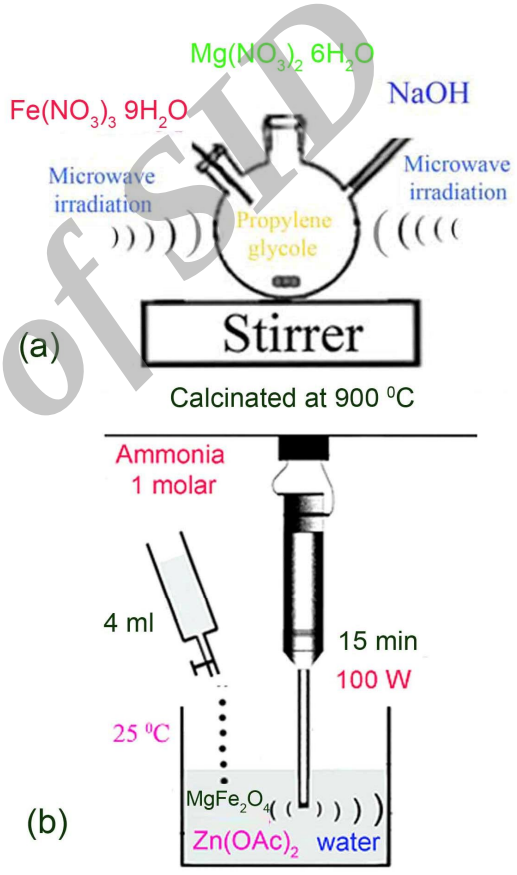

Fig. 1. Schematic of microwavepreparation of (a) $MgFe_2O_4$ nanoparticles (b) $MgFe_2O_4$-ZnO nanocomposite

The XRD pattern of ZnO nanoparticles is illustrated in Fig. 3. The pattern of ZnO nanoparticles confirms a pure hexagonal phase which is very close to the literature values (JCPDS No. 79-0208). The sharp peaks approve high crystalinity of the zinc oxide nanoparticles.

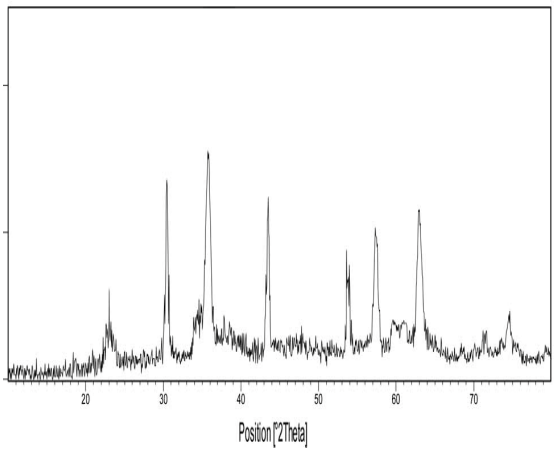

Fig. 2. XRD pattern of the $MgFe_2O_4$ nanoparticles

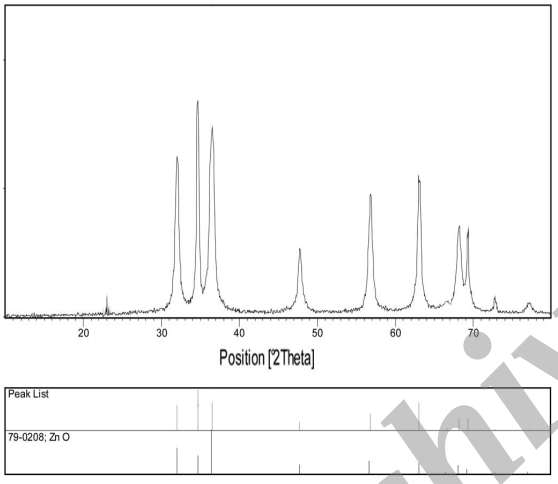

Fig. 3. XRD pattern of the ZnO nanoparticles

Fig. 4 illustrates SEM images of synthesized $MgFe_2O_4$ nanoparticles that confirm average diameter size of product is less than 40 nm.

SEM images of ZnO are studied and illustrated in Fig.5. According to images particles with average diameter about 20nm were synthesized.

During the ultrasound cycles, the cavitation bubbles would collapse, forming micro-jets that instantaneously generate intense local heating and high pressure. The micro-jet impact can develop pressures of about 2×10^8 Pa, and a local heating and cooling rate above 10^9 K/s. In fact, cavitation damage is generated by the non-spherical symmetric collapse of a cavitation bubble, either at or near a solid surface. Violent collapse of bubbles in asymmetrical geometries occur in a number of situations of practical interest including cavitation, shock-wave and laser lithotripsy [14,16].

Both microwave and ultrasonic methods propose easy manipulation in particle size and so magnetic properties by a simple change in power of pulsation and time of irradiation.

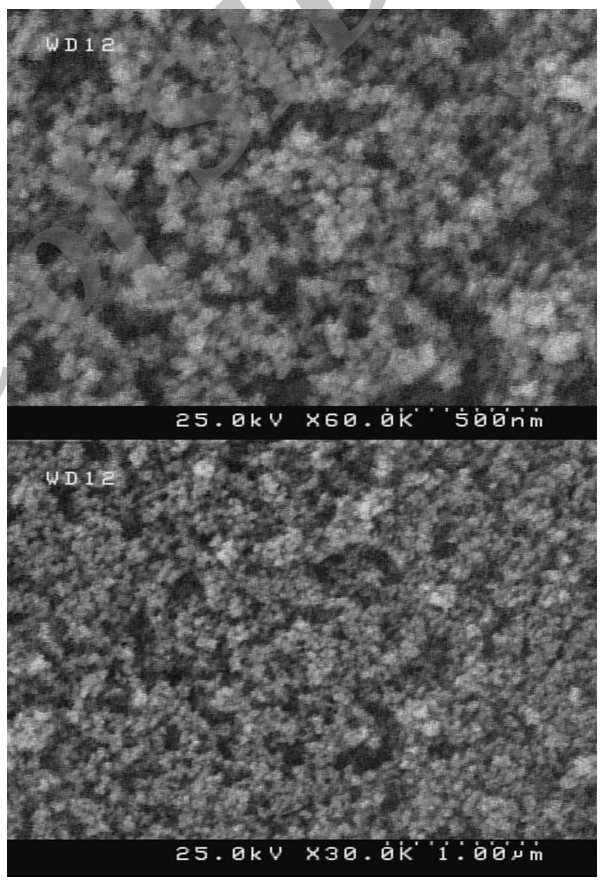

Fig. 4. SEM images of $MgFe_2O_4$ nanoparticles

Fig. 6 illustrates SEM images of $MgFe_2O_4$-ZnO nanocomposite and confirms some agglomeration compare to zinc oxide. It seems with calcination growth stage is predominant compare to nucleation stage.

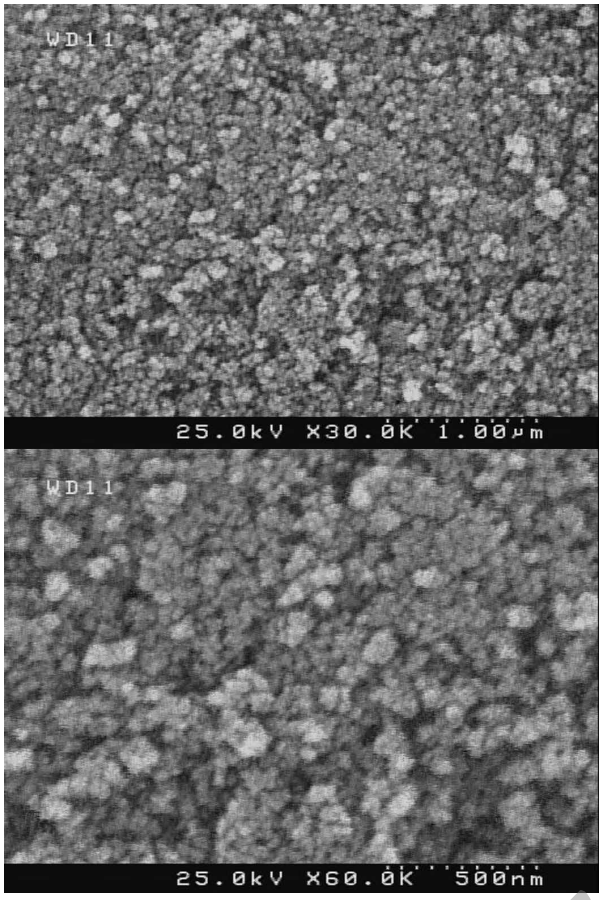

Fig. 5. SEM images of ZnO nanoparticles

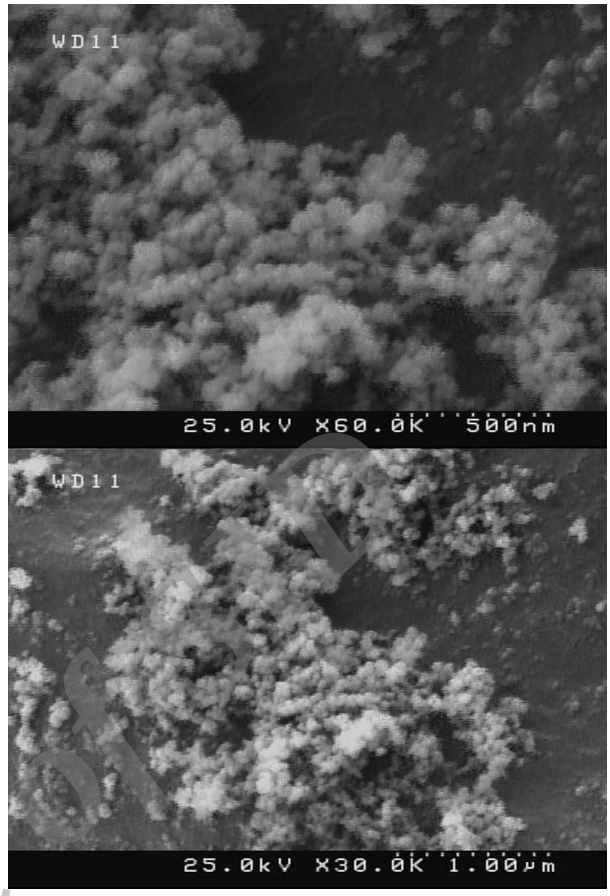

Fig. 6. SEM images of $MgFe_2O_4$-ZnO nanocomposite

The image shows that the sample consists of larger particles compare to pure ferrite nanoparticles.

Room temperature magnetic properties of samples are studied using a VSM device. Hysteresis loop of ferrite nanoparticles is depicted in Fig. 7.

$MgFe_2O_4$ synthesized nanoparticles show ferromagnetic behavior and have a saturation magnetization of 29 emu/g and coercivity about 83 Oe.

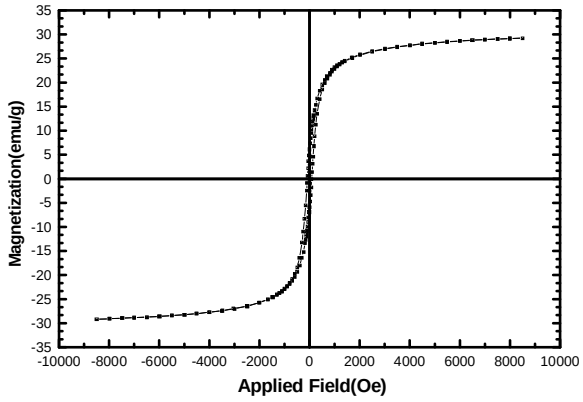

Fig. 7. Hysteresis curve of $MgFe_2O_4$ nanoparticles

Fig. 8 shows magnetization curve of $MgFe_2O_4$–ZnO nanocomposites that also exhibits ferromagnetic behavior with a coercivity around 102 Oe and a saturation magnetization of 15.6

emu/g. As expected due to presence of zinc oxide, its magnetization is lower than pure $MgFe_2O_4$ nanoparticles.

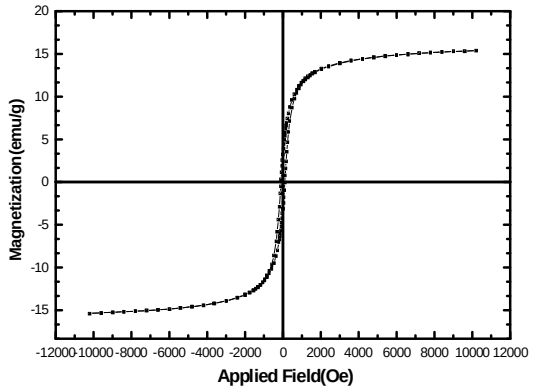

Fig. 8. Magnetization curve of $MgFe_2O_4$-ZnO nanocomposite

Fourier transform infra-red (FT-IR) spectrum of synthesized nanoparticles was recorded in the range of 400–4000 cm^{-1} and result is shown in Fig. 9. Absorption peaks around 438 and 618 cm^{-1} are related to metal-oxygen Mg-O and Fe-O bonds. The spectrum exhibits broad absorption peaks between 3500-3600 cm^{-1}, corresponding to the stretching mode of O-H group of Mg-Fe and also hydroxyl group that are adsorbed on the surface of nanoparticles.

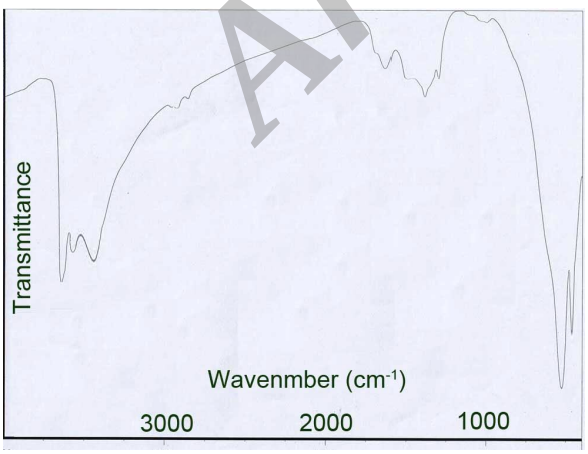

Fig. 9. FT-IR spectrum of $MgFe_2O_4$-ZnO nanocomposite

The photo-catalytic activity of the nanocomposite was evaluated by monitoring the degradation of methyl orange (MeO) in an aqueous solution. 0.1 g of magnetic nanocomposite was dispersed in 10 ml of MeO solution (5ppm). Pure methyl orange and MeO under UV irradiation in the presence of $MgFe_2O_4$-ZnO (40, 80 and 120 min) are illustrated in Fig 10a.

As time increased, more and more MeO were adsorbed on the magnetic nanocomposite catalyst, until the absorption peak (λ = 510 nm) vanish. The MeO concentration decreased rapidly with increasing time, and the peak almost disappeared after 120 min [1,17,18]. UV-visible spectra of pure methyl orange and methyl orange in presence of nanoparticles are shown in Fig 10b respectively.

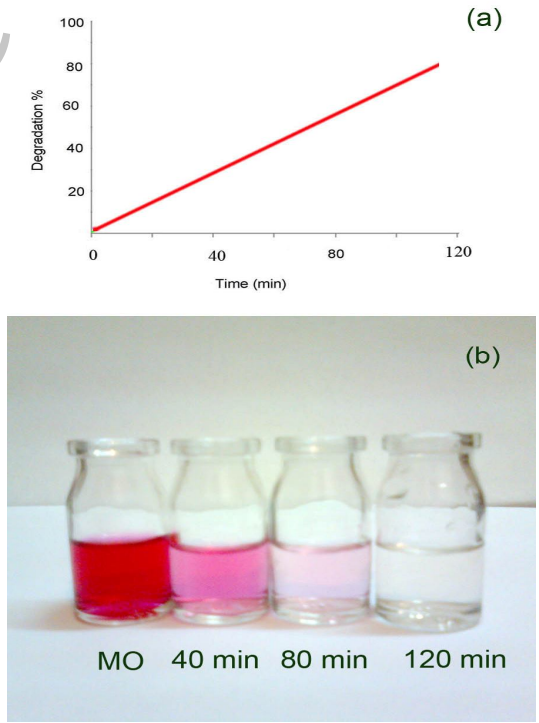

Fig. 10. Effect of $MgFe_2O_4$-ZnO under UV irradiation (a) Methyl orange (b) 40 min (c) 80 min (d) 120 min

4. Conclusion

Magnesium ferrite nanoparticles were synthesized via a microwave-assisted method. For synthesis $MgFe_2O_4$ the product was calcinated at 900 ºC for 2h. Then ZnO shell was synthesized on the ferrite-core via ultrasonic procedure. Vibrating sample magnetometer confirms nanoparticles and nanocomposites exhibit ferromagnetic behavior. The photocatalytic behavior of $MgFe_2O_4$-ZnO nanocomposite was evaluated using the degradation of a methyl orange aqueous solution under UV light irradiation. The results show that $MgFe_2O_4$-ZnO nanocomposite is promising materials with suitable performance in photo-catalytic applications.

Acknowledgments

This work has been supported financially by Arak University Research Council (AURC) under the grant number of 93/4656 [5-6-93]. The authors acknowledge AURC for the financial support.

References

[1] G. Nabiyouni, D. Ghanbari, S. Karimzadeh, B. Samani-Ghalehtaki, J Nano Struc. 4 (2014) 467-474.

[2] J. Saffari, N. Mir, D. Ghanbari, K. Khandan-Barani, A. Hassanabadi, M R Hosseini-Tabatabaei (in press 2015) DOI 10.1007/s10854-015-3622-y

[3] H.R. Momenian, M. Salavati-Niasari, D. Ghanbari, B. Pedram, F. Mozaffar, S. Gholamrezaei, J Nano Struc. 4 (2014) 99-104.

[4] F. Zhang, S. Kantake, Y. Kitamoto, M. Abe, IEEE Trans. Magn. 35 (1999) 2751–2753.

[5] Y. Kitamoto, S. Kantake, S. Shirasaki, F. Abe, M. Naoe, J. Appl. Phys. 85 (1999) 4708-4710.

[6] A.E. Berkowitz, W. Schuele, J. Appl. Phys. 30 (1959) 134–135.

[7]. D. Ghanbari, M. Salavati-Niasari, M. Ghasemi-Koch, J Indus Eng Chem. 20 (2014) 3970-3974.

[8] K. Maaz, A. Mumtaz, S.K. Hasanain, A. Ceylan, J. Magn. Magn. Mater 308 (2007) 289-295.

[9] X. Chu, D. Jiang, Y. Guo, C. Zheng, Sens. Actuator B. 120 (2006) 177.-181.

[10] C.C. Wang, I.H. Chen, C.R. Lin, J. Magn. Magn. Mater. 304 (2006) 451-453.

[11] Y.I. Kim, D. Kim, C.S. Lee, Phys. B 337 (2003) 42-51.

[12] Y. Shi, J. Ding, H. Yin, J. Alloys Compd. 308 (2000) 290-295.

[13] S. Gholamrezaei, M. Salavati-Niasari, D. Ghanbari, J Indus Eng Chem. 20 (2014) 3335-3341.

[14] P. Jamshidi, M. Salavati-Niasari, D. Ghanbari, H.R. Shams, J Clust Sci. 24 (2013) 1151-1162.

[15] S. Gholamrezaei, M. Salavati-Niasari, D. Ghanbari, J Indus Eng Chem. 20 (2014) 4000-4007.

[16] H.R. Momenian, S. Gholamrezaei, M. Salavati-Niasari, B. Pedram , F. Mozaffar , D. Ghanbari, J Clust Sci. 24 (2013) 1031-1042.

[17] A. Esmaeili-Bafghi-Karimabad, D. Ghanbari, M. Salavati-Niasari, L. Nejati-Moghadam, S. Gholamrezaei, J. Mater. Sci. Mater. Electron. 26 (2015) 6970-6977.

[18] L. Nejati-Moghadam, D. Ghanbari, M. Salavati-Niasari, A. Esmaeili-Bafghi-Karimabad , S. Gholamrezaei, J. Mater. Sci. Mater. Electron. 26 (2015) 6075-6083.